IEEE INSTRUMENTATION & MEASUREMENT SOCIETY

Received 31 May 2022; revised 18 July 2022; accepted 22 July 2022. Date of publication 29 July 2022; date of current version 10 August 2022.
The review of this paper was arranged by Associate Editor Marco Parvis.

Digital Object Identifier 10.1109/OJIM.2022.3194902

Toward Online Removal of Cardiac Interference From Trunk Electromyography by Morphological Modeling of the Electrocardiography

RUNWEI LIN [1], YICHAO WU [1], ZUYU DU [1], KAICHEN WANG [1], YANG YAO [1] (Member, IEEE), AND LIN XU [1,2] (Senior Member, IEEE)

[1]School of Information Science and Technology, ShanghaiTech University, Shanghai 201210, China

[2]Shanghai Engineering Research Center of Energy Efficient and Custom AI IC, Shanghai 201210, China

CORRESPONDING AUTHOR: L. XU (e-mail: xulin1@shanghaitech.edu.cn)

This work was supported in part by the National Natural Science Foundation of China under Grant 62171284, and in part by the Start-Up Funding from the ShanghaiTech University.

(Runwei Lin and Yichao Wu contributed equally to this work.)

ABSTRACT Trunk electromyography (EMG) has been widely used in many biomedical applications, which is usually contaminated by electrocardiography (ECG) interference. Several methods have been proposed for ECG removal from trunk EMG. However, most of them are either inaccurate or unsuitable for online applications, e.g., prosthesis control. The aim of the present study is therefore to develop an accurate ECG removal algorithm suitable for online applications. Each ECG wave was modeled by Gaussian kernel functions and subtracted from the trunk measurement to obtain a clean EMG. Two synthetic datasets were generated by mixing a real EMG with a healthy ECG and a dysrhythmia ECG, respectively. Average rectified value (ARV) and mean frequency (MF) were calculated from the reconstructed EMG and the clean EMG for performance evaluation. Moreover, real trunk EMG was recorded under isometric contractions with different forces. Correlation coefficient (CC) between the amplitude of the reconstruct EMG and the contraction force was calculated as performance metric. Small root mean square errors were observed in ARV and MF between the clean EMG and reconstructed EMG, i.e., 2.5 ± 0.7 μv and 2.0 ± 0.4 Hz for the synthetic dataset containing healthy ECG and 3.1 ± 1.7 μv and 3.0 ± 1.2 Hz for that containing dysrhythmia ECG. High CC (0.91 ± 0.12) between EMG amplitude and contraction force was observed for real trunk EMG. Our algorithm outperforms many of the state-of-the-art algorithms and is implemented in each cardiac cycle, enabling possible online applications such as prosthesis control.

INDEX TERMS Trunk electromyography, cardiac interference removal, electrocardiography modeling, Gaussian kernel functions.

I. INTRODUCTION

SURFACE electromyography (sEMG) is a measure of the electrical activity generated by the skeletal muscles during contraction. It can be nonabrasively recorded on the skin above the muscles, reflecting the functional state of related muscles. sEMG is therefore widely employed in many biomedical applications, such as the investigation of the neuromuscular systems [1], studies of biomechanics [2], controlling of myoelectric prosthesis [3], [4], and monitoring of respiration, stress, and epilepsy [5]–[7]. In some applications, e.g., prosthesis control and respiratory monitoring, sEMG has to be recorded from trunk muscles, such as pectoralis, diaphragm, and intercostal muscles [8]–[11].

Unfortunately, trunk EMG is usually contaminated by electrocardiography (ECG) [12], [13]. In trunk EMG measurement, this interference is unnegligible due to the low signal-to-noise ratio (SNR) between EMG and ECG, i.e., around -10 to -20 dB [14]. R peaks of ECG can be

clearly observed in trunk EMG [15]. It is difficult to separate these two signals by simple frequency-selective filtering approaches since their frequencies overlap in a very wide range, e.g., 20-100 Hz [16]. The ECG interference hampers strongly the practical applications of trunk EMG and, therefore, needs to be carefully removed before further analysis.

A number of algorithms have been proposed for the offline removal of ECG interference from trunk EMG. Gating (GT) [17] and high pass filtering (HPF) [18] are simple and most widespread methods in clinical practice. GT detects the R peaks in contaminated EMG and then sets the samples within the QRS interval, usually around 0.1s [17], to zero. This strategy will obviously lead to loss of EMG components in the QRS interval, particularly for high heart rates. HPF, typically with a cutoff frequency of 30 Hz, is also suggested to remove the ECG interference from trunk EMG [18]. However, the intrinsic limitation on frequency overlap makes it impossible to separate ECG and EMG components completely.

Template subtraction (TS), as firstly introduced in [19], is a more advanced algorithm for ECG interference removal from trunk EMG. TS method first builds an ECG template by aligning and averaging several QRS waveforms based on the assumptions that EMG is Gaussian distributed with zero mean and ECG is quasi-periodic [14], [20]. Clean EMG is then extracted by subtracting the obtained template from the original signal.

Blind source separation (BSS), such as singular value decomposition (SVD), principle component analysis (PCA), and independent component analysis (ICA), has also been investigated for ECG interference cancellation [15], [21], particularly in multichannel settings. ICA is popular in EMG denoising under the assumption that EMG and ECG are independent [15], [22], [23]. However, automatic identification of the noise components related to ECG is challenging [15]. Besides, the BBS method generally requires multichannel input signals, and not applicable to single channel recording. A recent study, however, proposed a single-channel based SVD method to remove ECG interference from trunk EMG with promising results [21].

Adaptive filtering (AF) and wavelet transform (WT) are widely used denoising techniques in many biomedical applications [24]–[26], and have also been introduced to eliminate ECG interference from trunk EMG [26], [27]. AF estimates the interference in each iteration and can be used for real-time applications. However, an appropriate reference signal correlated with ECG is necessary for AF, which is usually recorded by additional sensors and therefore complicates the measurement setup [15], [22], [28]. For WT, the main challenge is the selection of an appropriate mother wavelet and the corresponding noise components [14], [16].

A recent comparative review using synthesis data suggests TS to outperform other algorithms as evidenced by better average rectified value (ARV) and mean frequency (MF) calculated from the reconstructed EMG [16]. However, the performance of the TS method depends strongly on two assumptions, i.e., quasi-periodic ECG and Gaussian distributed EMG with zero mean, which are not always satisfied. In fact, decreased performance is observed for TS when EMG is contaminated by abnormal, e.g., dysrhythmia ECG [16]. Besides, TS method needs to average several QRS complexes and may not be suitable for online applications such as prosthesis control.

The aim of the present study is therefore to develop an accurate algorithm for ECG-interference removal from trunk EMG that is suitable for online applications. To this end, ECG waveform in each cardiac cycle was estimated by dedicated morphological modeling and then subtracted from the original signal to reconstruct the clean EMG. In fact, many models have been proposed for the cardiac activity [29], [30], among which the Gaussian-kernel-based dynamical model (GKDM) is simple but shows promising results [29]–[31]. The GKDM is therefore employed in the present study in order to model the ECG interference.

The proposed GKDM-based ECG interference removal algorithm was evaluated by synthetic trunk EMG as well as real trunk EMG measurement under isometric contraction at different levels. ARV and MF were calculated from the reconstructed EMG and compared with that from the clean EMG in order to assess the performance of the proposed method on the synthetic datset. Correlation coefficient between the amplitude of the reconstructed EMG, i.e., ARV, and the contraction force was calculated as performance metric for real trunk EMG. Besides, the performance of the proposed method was compared with the state-of-the-art algorithms, such as GT, TS, WT, and ICA.

II. MATERIALS AND METHODS

A. MORPHOLOGICAL MODELING OF ECG

A general idea to model the morphology of an ECG signal is to express the ECG, denoted as $\hat{x}(t)$, as linear combination of a set of basis functions $\psi_i(t)$, as given by [30]

$$\hat{x}(t) = \sum_{i=1}^{N} a_i \cdot \psi_i(t), \tag{1}$$

where a_i is the amplitude of the i^{th} basis function and N the number of adopted basis functions. An orthogonal basis function, such as sinusoidal, is widely used since it is mathematically irredundant, and a_i conveys information about the relevance of each basis function in constructing $\hat{x}(t)$ [30]. However, given the specific morphology, a more straightforward and meaningful approach to model an ECG is to decompose it into the well-known P, QRS, and T waves, which can be modeled as Gaussian basis functions [32]. A single ECG beat is therefore modeled as

$$\hat{x}(t) = \sum_{i=1}^{N} a_i \cdot \exp\left[-\frac{(t-t_i)^2}{2b_i^2}\right], \tag{2}$$

where t_i and b_i are the center and width of the i^{th} Gaussian basis function, respectively.

In order to model multiple ECG beats with arbitrary heart rates, the cardiac phase signal, denoted as $\theta(t)$, is usually employed to time-scale all ECG beats irrespective of the beat-to-beat variations of the heart rate. The cardiac phase $\theta(t)$ is defined as a monotonically increasing function, ranging from $-\pi$ to $+\pi$ [33]. It is assigned to each ECG beat with the R-peak fixed at $\theta(t) = 0$ and the starting and ending points of the ECG beat at $\theta(t) = -\pi$ and $+\pi$, respectively.

Using the cardiac phase, the ECG model in (2) can be expressed as

$$\hat{x}(t) = \sum_{i=1}^{N} a_i \cdot \psi_i[\theta(t)], \tag{3}$$

where

$$\psi_i[\theta(t)] = \exp\left\{-\frac{[\theta(t) - \theta_i]^2}{2b_i^2}\right\}. \tag{4}$$

The cardiac phase $\theta(t)$ is time-varying and related to the heart rate by

$$\frac{d}{dt}\theta(t) = 2\pi f(t), \tag{5}$$

where $f(t)$ is the heart rate in Hz and can fluctuate over time. Multiple beats with arbitrary heart rates are then achieved by updating $\theta(t)$ using the dynamic in (5). Furthermore, by augmenting the cardiac phase dynamic in (5) with the dynamics of (4), a unified dynamic model generating multiple ECG beats is obtained, as given by [30]

$$\begin{cases} \hat{x}(t) = \sum_{i=1}^{N} a_i \cdot \psi_i[\theta(t)]. \\ \frac{d}{dt}\psi_i[\theta(t)] = -\psi_i[\theta(t)] \cdot \frac{\theta(t)-\theta_i}{b_i^2} \cdot \frac{d}{dt}\theta(t). \\ \frac{d}{dt}\theta(t) = 2\pi f(t). \end{cases} \tag{6}$$

The interpretation of the Gaussian kernel model is straightforward since each Gaussian kernel can correspond to one of the P, QRS, and T waves of the ECG. Each Gaussian kernel has multiple degrees of freedom, i.e., a_i, b_i, and θ_i, which can be obtained by minimizing the energy of the residual error signal between the observation $x(t)$ and the synthesised signal by the model, as given by

$$En = \int_{-\pi}^{\pi} |e(t)|^2 = \int_{-\pi}^{\pi} \left| x(t) - \sum_{i=1}^{N} a_i \cdot \psi_i[\theta(t)] \right|^2. \tag{7}$$

A nonlinear least squares algorithm is required to find the minimum value of E_n due to the nonlinear relationship between $\hat{x}(t)$ and the model parameters [34]. An alternative approach that can be employed to identify the model parameters is the expectation maximization method [35].

B. ECG INTERFERENCE REMOVAL FROM TRUNK EMG

In the present study, the dynamic ECG model is employed to remove the cardiac interference from trunk EMG. The scheme of the whole process is shown in Fig. 1, in which ECG is considered as additive noise, in line with previous studies [16], [21]. An ECG waveform is first estimated by the model, whose parameters are optimized by minimizing the least square error between the raw data and the output of the model. The obtained ECG template is then subtracted from the raw data in order to eliminate the cardiac interference.

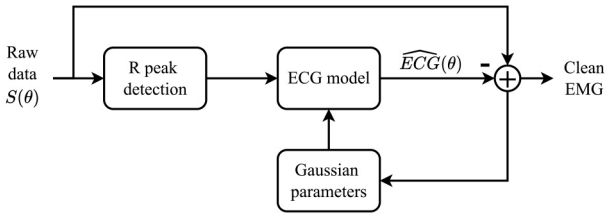

FIGURE 1. Scheme of the proposed ECG interference removal algorithm.

Considering possible online requirement for trunk EMG applications, e.g., prosthesis control, the removal of the cardiac interference is implemented in each cardiac cycle in the present study. To this end, the R peaks of the ECG interference are first identified. The whole signal is then split into individual segments containing only one beat in each. Specifically, each single beat segment is determined by the time interval $[(t_j - 0.5t_{Rj}) \quad (t_j + 0.5t_{Rj})]$, where t_j denotes the time of the j^{th} R peak, and t_{Rj} represents the corresponding R-R interval. The identified single ECG beat is then mapped to the cardiac phase with the R-peak, the starting and ending points fixed at $\theta(t) = 0$, $-\pi$, and π, respectively.

The Gaussian kernel model in (3) and (6) is then employed to estimate the ECG interference, i.e., $\widehat{ECG}(\theta)$. According to (7), model parameters, i.e., a_i, b_i, and θ_i, are obtained by

$$[a_i, b_i, \theta_i] = \arg\min_{a_i, b_i, \theta_i} |\widehat{ECG}(\theta) - ECG(\theta)|^2, \tag{8}$$

where $ECG(\theta)$ is a clean reference ECG, which is unfortunately unavailable since the original recording is a mixture of EMG and ECG signals. However, it is reasonable to assume that the EMG and ECG signals are independent given their different physiological origins. Consequently, minimization of the least square between $\widehat{ECG}(\theta)$ and $ECG(\theta)$ is equivalent to the minimization of the least square between $\widehat{ECG}(\theta)$ and the mixture $S(\theta)$,

$$[a_i, b_i, \theta_i] = \arg\min_{a_i, b_i, \theta_i} \left|\widehat{ECG}(\theta) - S(\theta)\right|^2. \tag{9}$$

It is reported that the model approximation error decreases very quickly by increasing the number of Gaussian kernels [30]. However, an increase in the kernel number will inevitably increase the complexity and thus the computational cost of the model. Since each Gaussian kernel can model one of the ECG sub-waves, e.g., P, Q, R, S, and T, six Gaussian kernels are employed in the present study, which is sufficient to cover all ECG sub-waves. This choice has also been verified by our experimental test. An example of the ECG signal estimated with six Gaussian kernel functions is shown in Fig. 2.

Furthermore, given the nonlinear relationship between the ECG signal and the model parameters, a nonlinear least

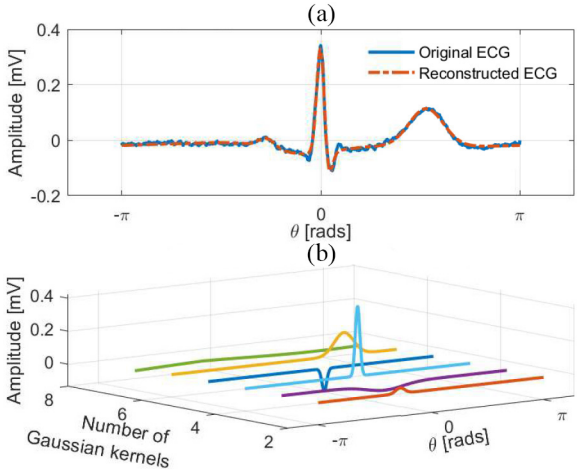

FIGURE 2. Example of ECG modeling by Gaussian kernel functions: a) the original and reconstructed ECG; b) Six Gaussian kernel functions used to model the ECG.

TABLE 1. Initial model parameters of the 6 Gaussian kernel functions.

Gaussian functions	1	2	3	4	5	6
θ_i(rads)	$-\pi/3$	$-\pi/12$	0	$\pi/12$	$2\pi/5$	$\pi/2$
a_i	1.2	-5	30	-7.5	1.2	1.2
b_i	0.25	0.1	0.1	0.1	0.2	0.2

square optimization approach described in [29] was adopted in the present study in order to optimize the model parameters. The initial values of the model parameters of the Gaussian kernel functions were taken from previous studies [29], [32], as given in Table 1 .The estimated ECG interference was then subtracted from the mixed recordings in order to obtained the clean EMG.

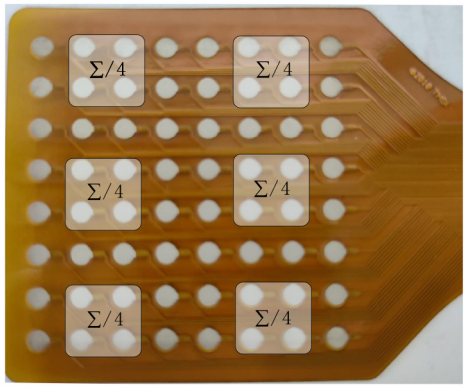

FIGURE 3. HD electrode grid and the subsets generating the six big EMG channels for the synthetic datasets.

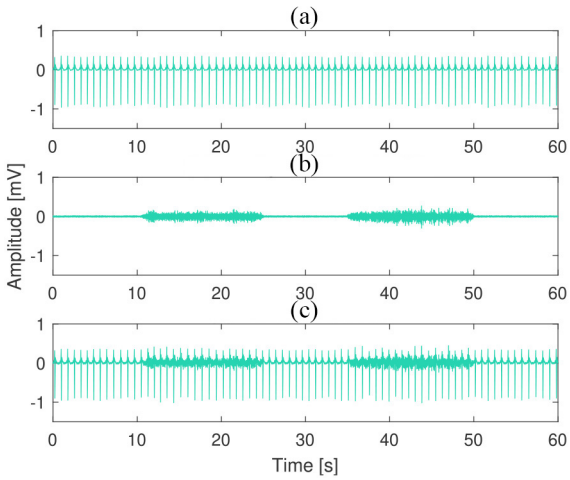

FIGURE 4. Example of synthetic trunk EMG: a) band-pass filtered ECG; b) band-pass filtered EMG; c) ECG and EMG mixture.

C. VALIDATION

1) DATA ACQUISITION AND PREPROCESSING

1) Synthetic trunk EMG: Two synthetic datasets were generated by mixing an EMG dataset with a healthy ECG and a dysrhythmia ECG, respectively, providing a ground truth to assess the performance of the proposed algorithm. Surface EMG was recorded on the biceps brachii of nine healthy subjects' dominant arm with a high-density (HD) electrode grid placed longitudinally to the muscle fibers. The HD grid consists of 64 (8 × 8) electrodes with diameter and inter-electrode distance of 4 mm and 8 mm, respectively, as shown in Fig. 3. An Ag/AgCl electrode (1 cm diameter) was placed on the subject's right clavicle as patient ground. A Refa amplifier (TMS International, Enschede) was employed to amplify and digitalize the recorded signals at a sampling frequency of 2048 Hz. Participants were seated with their back straight and elbow joint at 90 degrees. The duration of the whole acquisition protocol was 60 s, including a 10-s rest, a 15-s isometric contraction at 50% of their maximal voluntary contraction (MVC), a 10-s rest, a 15-s 50% MVC, and a 10-s rest. The experimental setup and further details on the acquisition protocol were described in our previous studies [16], [36]. This protocol was approved by the Ethical Committee of the Máxima Medical Center (Veldhoven, the Netherlands).

The ECG signals were derived from the PTB Diagnostic ECG Database [37]. Nine healthy datasets and nine datasets with dysrhythmia were randomly selected. Among the 15 signals in each dataset, the precordial leads (v1-v6) positioned on the chest with respect to the Wilson's central terminal were chosen to mimic ECG interference in trunk EMG measurement. All ECG datasets were sampled at 1000 Hz.

In order to match the adopted number of ECG channels, six big EMG channels were extracted with each being the average of a subset of four neighbor channels of the HD grid, as shown in Fig. 3. The extracted EMG signals were downsampled to 1000 Hz to match the sampling frequency of the ECG signals. A second-order infinite response filter was employed to eliminate the power-line interference in both EMG and ECG. A third order Butterworth band-pass filter

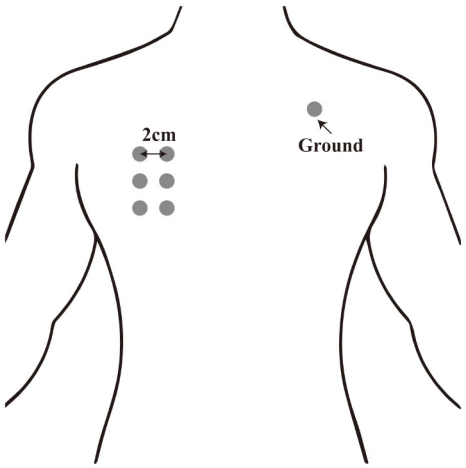

FIGURE 5. Electrode position for real trunk EMG recording.

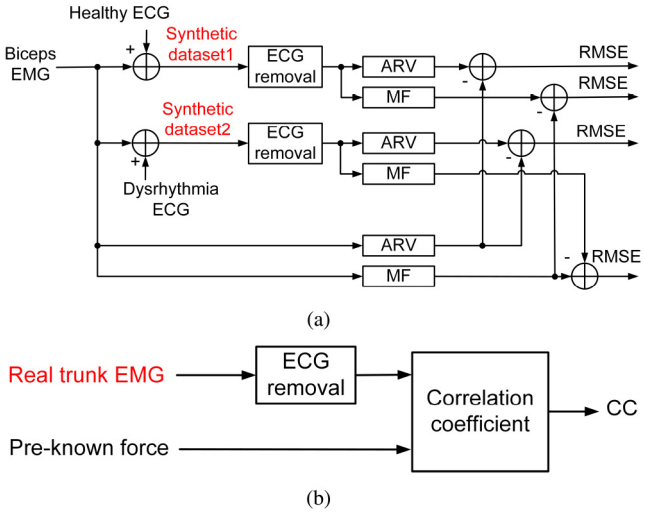

FIGURE 6. Processing chain for different datasets: a) synthetic datasets; b) real trunk EMG.

was applied to remove the noise outside the frequency band of interest, i.e., 10 to 500 Hz for EMG and 1 to 120 Hz for ECG [16], [38]. Two synthetic datasets were generated by mixing the EMG with healthy ECG and dysrhythmia ECG, respectively, in which the EMG was re-scaled to obtain a realistic SNR with respect to the ECG, e.g., −10 dB [14].

2) Real trunk EMG: Real trunk EMG was also collected on the right pectoralis of nine healthy male subjects. As shown in Fig. 5, six Ag/AgCl electrodes were placed on the pectoralis with inter-electrode distance of 2 cm. The patient ground was placed on the subject's right clavicle. The same Refa amplifier was used to record the data at 2048 Hz.

Similar to Section II-C1a, the participants were required to sit on a bench with their back straight and elbow joint at 90 degrees. They performed five trials of isometric contraction with different levels of constant load, i.e., 20%, 30%, 40%, 50%, and 60% of their MVC. Each trail lasted for 15 seconds, separated by a 3-min rest period in order to avoid muscle fatigue.

For each recording, the first and last two seconds were abandoned to avoid transient effects, resulting in a 11-s trunk EMG recording. No re-referencing was performed and thus the six EMG channels were referenced to their average [39], guaranteed by the hardware of the adopted Refa amplifier. The collected sEMG were then band-pass filtered between 10 and 500 Hz using a third-order Butterworth filter. The same second-order notch filter as used in Section Section II-C1a was applied to eliminate the power-line interference.

2) PERFORMANCE METRICS

The proposed GKDM-based ECG removal method was evaluated with both synthetic datasets and real trunk EMG. The whole processing chain for different datasets are illustrated in Fig. 6.

For the two synthetic datasets, two commonly used criteria, i.e., ARV and MF [16], [40], were employed as performance metrics. For each channel of the dataset, ARV was calculated on a non-overlap 1-s sliding window over the entire 60-s signal, and MF was calculated using the same sliding window but only on the two contraction periods, i.e., 10-25 s and 35-50 s, in line with [16]. The root mean square error (RMSE) between ARV and MF calculated from the reconstructed EMG and that from the clean EMG was computed for each channel. The average RMSE in ARV and MF over the six channels was consider for each subject.

For real trunk EMG, however, a clean reference EMG is not available, and therefore RMSE in ARV and MF can not be obtained. Yet many studies have reported a strong correlation between EMG amplitude and contraction force [8], [14], [41]. And this correlation may be nonlinear for big muscles such as pectoralis [41]. Accordingly, a second-order polynomial was employed to fit the relationship between the EMG amplitudes estimated in different trials and the corresponding contraction forces for each subject. The correlation coefficient (CC) of the polynomial fitting was adopted to assess the efficiency of ECG-interference removal, with higher CC indicating better ECG removal. For each trial, the EMG amplitude was estimated by the average of ARVs calculated from the reconstructed EMG in different channels.

D. COMPARISON WITH ALTERNATIVE ALGORITHMS

The proposed GKDM-based ECG removal algorithm were compared with some of the state-of-the-art algorithms reported in the literature, such as GT, TS, WT, and ICA. These alternative methods were implemented in the same way as [16]. For the two synthetic datasets, the RMSEs in ARV and MF of the nine subjects were adopted for the comparison among different methods. For real trunk EMG, CCs of different subjects were utilized for comparison. The one-sample Kolmogorov-Smirnov test indicated that the data are normally distributed. Data are therefore presented as mean ± standard deviation (SD). A one-way ANOVA was employed to determine the global difference in the mean values among different algorithms. A post hoc analysis using the least

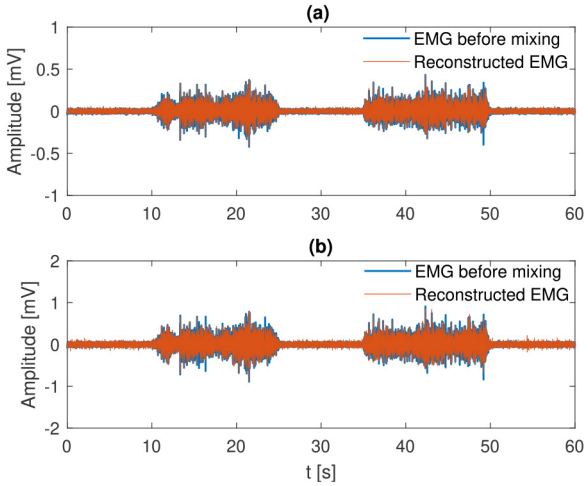

FIGURE 7. Example of the reconstructed EMG from the synthetic datasets: a) EMG + healthy ECG; b) EMG + dysrhythmia ECG.

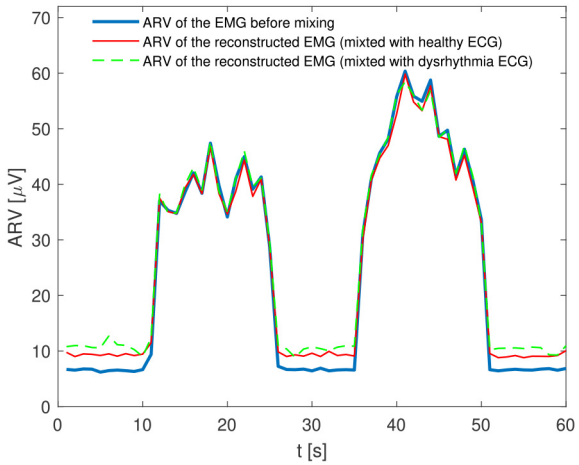

FIGURE 8. Example of ARV calculated from the EMG signals shown in Fig. 7.

TABLE 2. RMSE results in ARV and MF for synthetic trunk EMG obtained with different methods.

	Dataset1[1]		Dataset2[2]	
	ARV [μv]	MF [Hz]	ARV [μv]	MF [Hz]
GT	6.5 ± 1.4	7.6 ± 3.8	8.5 ± 8.2	6.9 ± 3.8
TS	2.7 ± 0.4	2.6 ± 0.5	4.1 ± 1.5	3.2 ± 0.7
WT	15.5 ± 2.9	6.7 ± 0.6	14.4 ±12.1	8.4 ± 1.3
ICA	4.1 ± 0.8	6.4 ± 1.8	6.3 ± 6.0	10.1 ± 7.6
Proposed	**2.5 ± 0.7**	**2.0 ± 0.4**	**3.1 ± 1.7**	**3.0 ± 1.2**

[1] Synthetic trunk EMG with healthy ECG.
[2] Synthetic trunk EMG with dysrhythmia ECG.

significant difference method was employed to test the difference between pairs of algorithms. The significant level was set at 0.05.

In addition, the execution time of different methods was determined in order to evaluate their computational complexity. Each algorithm was repeated ten times and the average execution time was taken into consideration. All the analysis was implemented in MATLAB 2019b (MathWorks, Natick, MA, USA) using a DELL Optiplex 7080 Tower PC (Dell Round Rock, TX, USA), with an Inter Core i9-10900K CPU @ 3.70 GHz (10 CPUs) processor (Inter, Santa Clark, CA, USA).

III. RESULTS

A. SYNTHETIC TRUNK EMG

Figure 7 shows a representative example of the reconstructed EMG obtained by the proposed GKDM-based ECG removal algorithm from the synthetic trunk EMG. It is clear that for both datasets, i.e., EMG + healthy ECG and EMG + dysrhythmia ECG, the reconstructed EMG are quite close to the clean EMG before mixing, indicating a very good performance of the proposed GKDM-based algorithm for cardiac interference removal.

Figure 8 shows an example of the ARV calculated from the EMG signals shown in Fig. 7. ARV is calculated using a 1-s sliding window with no overlap. During the three rest segments, a slight difference was observed in ARV between the clean EMG and the reconstructed EMG, possibly due to the measurement noise presented in the rest period. However, during the two contraction segments, ARV calculated from the reconstructed EMG matches that from the clean EMG very well, irrespective the synthetic dataset consisting of healthy or dysrhythmia ECG. An example of MF calculated from the same EMG signals using the same sliding window is shown in Fig. 9. MF is calculated on the contraction segments of the reconstructed EMG, which are quite close to that obtained from the clean EMG for both synthetic datasets.

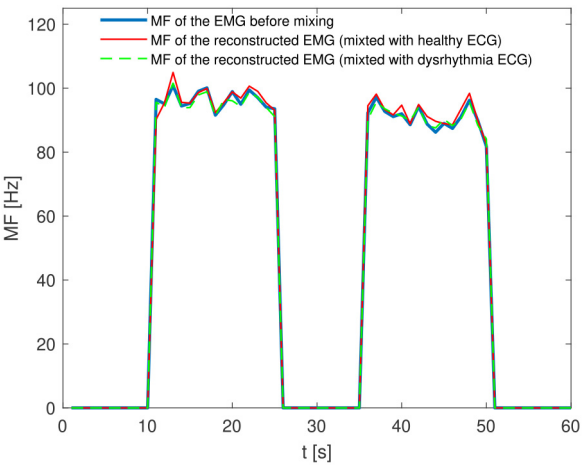

FIGURE 9. Example of MF calculated from the same EMG signals as ARV.

The average (over 9 subjects) RMSE results in ARV and MF between the reconstructed EMG and the clean EMG

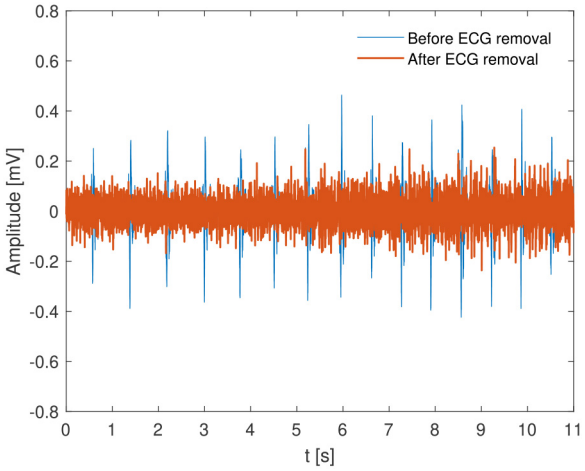

FIGURE 10. Example of the reconstructed EMG from real trunk EMG measurement.

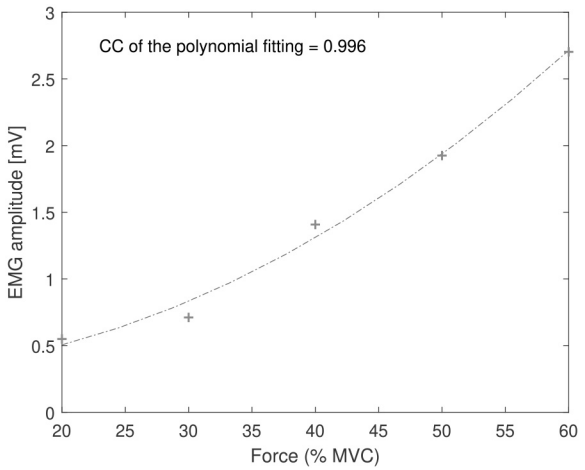

FIGURE 11. Example of the polynomial fitting between EMG amplitude and force.

derived with different ECG removal methods are summarized in Table 2. Our statistical analysis shows TS and the proposed method to produce significantly ($p < 0.05$) smaller RMSEs than other three methods for both synthetic datasets. In fact, our method produces the smallest RMSE. Unfortunately, difference between our method and TS is not statistically significant. However, while applied to the dataset consisting of dysrhythmia ECG, clearly performance decay is observed for TS.

B. REAL TRUNK EMG

An example of the reconstructed EMG from real trunk EMG measurement is shown in Fig 10. It is clear that the ECG interference has been effectively removed. Figure 11 shows an example of the second-order polynomial fit between the amplitude of the reconstructed EMG and the contraction force. A very high CC is observed for the fitting, i.e., 0.996, suggesting an excellent removal of the cardiac interface for the proposed ECG removal algorithm.

The average (over 9 subjects) CC results obtained with different ECG removal methods are reported in Table 3. An

TABLE 3. Correlation coefficient results of different methods together with their execution time (mean ± SD).

	Real trunk EMG	Execution time
	Correlation coefficient	[ms] / cardiac cycle
GT	0.90 ± 0.12	0.02 ± 0.02
TS	0.90 ± 0.13	0.78 ± 0.05
WT	0.90 ± 0.12	0.19 ± 0.02
ICA	0.84 ± 0.12	0.33 ± 0.11
Proposed	**0.91 ± 0.12**	**34.1 ± 3.5**

average CC above 0.9 is achieved by all methods except for ICA. Our method produces the highest CC but, unfortunately, no significant difference can be determined among different algorithms. The execution time of different methods is also reported in Table 3.

IV. DISCUSSION

The present study aims at developing an accuracy algorithm suitable for online removal of cardiac interference from trunk EMG measurement. To this end, ECG waveform is estimated in each cardiac cycle by dedicated modeling with Gaussian kernel functions. The estimated ECG waveform is then subtracted from the original data in order to obtain an EMG without ECG interference.

Although the employed Gaussian kernel functions are non-orthogonal and therefore mathematically redundant, each Gaussian function can correspond to a typical ECG sub-wave such as P, Q, R, S, and T, providing a straightforward and meaningful interpretation for the proposed method for ECG modeling. Studies have indicated an increase in the accuracy of the ECG model with increased number of Gaussian kernels [30]. However, an increase in the number of Gaussian functions will inevitably increase the complexity and thus the computational time of the model, i.e., $O(3N^2)$ for one kernel [29], hampering the applicability of the proposed method for online application scenarios. Given the fact the an ECG cycle is will defined by several typical sub-waves, six Gaussian functions should be sufficient and therefore adopted in the present study for ECG modeling. This choice is confirmed by the simulation shown in Fig. 2 as well as the excellent results in our dedicated evaluation.

The proposed GKDM-based ECG removal algorithm is first evaluated by two synthetic datasets, i.e., EMG + healthy ECG and EMG + dysrhythmia ECG, in which ARV and MF are adopted as performance metrics [14]. Though this approach, a clean EMG before mixing is available, enabling quantitative assessment of the proposed ECG removal method with a ground truth. Worthily to note that the ECG and EMG used in the synthetic datasets are all from real measurements, including possible noise from the instrumentation and the environment. Besides, the SNR between

EMG and ECG in the synthetic datasets is realistic [14]. The synthetic datasets can therefore be considered reliable for evaluating the performance of the proposed method.

The RMSE results obtained from the synthetic datasets suggest the proposed method to outperform all other methods except for TS. However, the performance of TS decreases clearly when the EMG is contaminated by abnormal ECG (Table 2), in line with [16]. This can be explained by the fact that one of the required assumptions for TS, i.e., quasi-periodic ECG, may be unsatisfied in abnormal ECG [16]. Furthermore, our method works in each cardiac cycle, and is, therefore, more suitable for online applications than TS, as TS requires the average of a number of ECG cycles, e.g., 6 to 10 [19]. In addition, instead of using the nonlinear least square [29], Kalman filter can also be employed for real-time optimization of the model parameters [42], leading to real-time application of the GKDM-based ECG removal algorithm.

While providing excellent ECG removal, the proposed method may be suitable for real-time applications. These are the main novelty and contributions of the present study. Worthily to note that AF method can also be used for real-time applications. However, the requirement of additional sensor to record a reference for AF complicates the measurement setup and increases the power consumption. Besides, the performance of AF is usually unsatisfactory due most probably to the fact that the acquisition of a clear reference ECG is very difficult [16].

The proposed method has also been evaluated by real trunk EMG measurement. However, the results observed in real trunk EMG measurement are inconsistent with that in the synthetic datasets, i.e., no significant performance difference is observed among different methods. This is most probably due to the adopted CC as performance metric is in fact a dilemma.

On the one hand, due to the lack of a ground truth in real trunk EMG measurement, CC between EMG amplitude and contraction force is employed as performance metric [8], [14], [41]. On the other hand, in order to calculate the correlation between EMG amplitude and contraction force, different levels of contraction force are required, i.e., 20% to 60% MVC in the present study, which are in fact usually higher than most of real trunk EMG scenarios, such as controlling of myoelectric prosthesis [3], [4] and monitoring of respiration, stress, and epilepsy [5]–[7]. The high contraction forces lead to increased EMG amplitude and thus decreased contribution of the residual ECG obtained with difference methods. As a consequence, the observed CC shows no significant difference among different methods.

V. CONCLUSION

In the present study, a GKDM-based method is proposed for cardiac interference removal from trunk EMG. The proposed method is evaluated by two synthetic datasets as well as a real EMG measurement. Our results show excellent performance of the proposed method for ECG interference removal, outperforming many of the state-of-the-art algorithms reported in the literature. Furthermore, the proposed ECG removal method is implemented in each cardiac cycle, enabling possible online application scenarios such as prosthesis control. The influence of the SNR between EMG and ECG on the performance of the proposed method may be interested for future studies. Clinical practice with very high real-time requirement may consider Kalman filter for the optimization of the parameters of the GKDM model.

REFERENCES

[1] X. Tang, X. Zhang, X. Gao, X. Chen, and P. Zhou, "A novel interpretation of sample entropy in surface electromyographic examination of complex neuromuscular alternations in subacute and chronic stroke," *IEEE Trans. Neural Syst. Rehabil. Eng.*, vol. 26, no. 9, pp. 1878–1888, Sep. 2018.

[2] M. A. Crary, G. D. Carnaby, and M. E. Groher, "Biomechanical correlates of surface electromyography signals obtained during swallowing by healthy adults," *J. Speech Lang. Hear. Res.*, vol. 49, no. 1, pp. 186–193, 2006.

[3] A. H. Al-Timemy, G. Bugmann, J. Escudero, and N. Outram, "Classification of finger movements for the dexterous hand prosthesis control with surface electromyography," *IEEE J. Biomed. Health Inform.*, vol. 17, no. 3, pp. 608–618, May 2013.

[4] A. H. Al-Timemy, R. N. Khushaba, G. Bugmann, and J. Escudero, "Improving the performance against force variation of EMG controlled multifunctional upper-limb prostheses for transradial amputees," *IEEE Trans. Neural Syst. Rehabil. Eng.*, vol. 24, no. 6, pp. 650–661, Jun. 2016.

[5] N. L. Vandenbussche, S. Overeem, J. P. van Dijk, P. J. Simons, and D. A. Pevernagie, "Assessment of respiratory effort during sleep: Esophageal pressure versus noninvasive monitoring techniques," *Sleep Med. Rev.*, vol. 24, pp. 28–36, Dec. 2015.

[6] U. Lundberg *et al.*, "Psychophysiological stress and EMG activity of the trapezius muscle," *Int. J. Behav. Med.*, vol. 1, no. 4, pp. 354–370, 1994.

[7] I. Conradsen, P. Wolf, T. Sams, H. B. D. Sorensen, and S. Beniczky, "Patterns of muscle activation during generalized tonic and tonic–clonic epileptic seizures," *Epilepsia*, vol. 52, no. 11, pp. 2125–2132, 2011.

[8] X. Zhang, X. Ren, X. Gao, X. Chen, and P. Zhou, "Complexity analysis of surface EMG for overcoming ECG interference toward proportional myoelectric control," *Entropy*, vol. 18, no. 4, p. 106, 2016.

[9] K. Tusiewicz, H. Moldofsky, A. C. Bryan, and M. H. Bryan, "Mechanics of the rib cage and diaphragm during sleep," *J. Appl. Physiol.*, vol. 43, no. 4, pp. 600–602, 1977.

[10] R. A. Stoohs, H.-C. Blum, L. Knaack, B. Butsch-von-der-Heydt, and C. Guilleminault, "Comparison of pleural pressure and transcutaneous diaphragmatic electromyogram in obstructive sleep apnea syndrome," *Sleep*, vol. 28, no. 3, pp. 321–329, 2005.

[11] E. Z. Hawkes, A. V. Nowicky, and A. K. McConnell, "Diaphragm and intercostal surface EMG and muscle performance after acute inspiratory muscle loading," *Respiratory Physiol. Neurobiol.*, vol. 155, no. 3, pp. 213–219, 2007.

[12] Y. Hu, J. N. F. Mak, and K. D. K. Luk, "Effect of electrocardiographic contamination on surface electromyography assessment of back muscles," *J. Electromyogr. Kinesiol.*, vol. 19, no. 1, pp. 145–156, 2009.

[13] G. T. Allison, "Trunk muscle onset detection technique for EMG signals with ECG artefact," *J. Electromyogr. Kinesiol.*, vol. 13, no. 3, pp. 209–216, 2003.

[14] P. Zhou and T. A. Kuiken, "Eliminating cardiac contamination from myoelectric control signals developed by targeted muscle reinnervation," *Physiol. Meas.*, vol. 27, no. 12, pp. 1311–1327, 2006.

[15] N. W. Willigenburg, A. Daffertshofer, I. Kingma, and J. H. Van Dieën, "Removing ECG contamination from EMG recordings: A comparison of ICA-based and other filtering procedures," *J. Electromyogr. Kinesiol.*, vol. 22, no. 3, pp. 485–493, 2012.

[16] L. Xu, E. Peri, R. Vullings, C. Rabotti, J. P. Van Dijk, and M. Mischi, "Comparative review of the algorithms for removal of electrocardiographic interference from trunk electromyography," *Sensors*, vol. 20, no. 17, p. 4890, 2020.
[17] T. W. Schweitzer, J. W. Fitzgerald, J. A. Bowden, and P. Lynne-Davies, "Spectral analysis of human inspiratory diaphragmatic electromyograms," *J. Appl. Physiol.*, vol. 46, no. 1, pp. 152–165, 1979.
[18] M. S. Redfern, R. E. Hughes, and D. B. Chaffin, "High-pass filtering to remove electrocardiographic interference from torso EMG recordings," *Clin. Biomech.*, vol. 8, no. 1, pp. 44–48, 1993.
[19] R. Bloch, "Subtraction of electrocardiographic signal from respiratory electromyogram," *J. Appl. Physiol.*, vol. 55, no. 2, pp. 619–623, 1983.
[20] A. Bartolo, R. R. Dzwonczyk, O. Roberts, and E. Goldman, "Description and validation of a technique for the removal of ECG contamination from diaphragmatic EMG signal," *Med. Biol. Eng. Comput.*, vol. 34, no. 1, pp. 76–81, 1996.
[21] E. Peri *et al.*, "Singular value decomposition for removal of cardiac interference from trunk electromyogram," *Sensors*, vol. 21, no. 2, p. 573, 2021.
[22] J. N. Mak, Y. Hu, and K. D. K. Luk, "An automated ECG-artifact removal method for trunk muscle surface EMG recordings," *Med. Eng. Phys.*, vol. 32, no. 8, pp. 840–848, 2010.
[23] M. Chen, X. Zhang, X. Chen, M. Zhu, G. Li, and P. Zhou, "FastICA peel-off for ECG interference removal from surface EMG," *Biomed. Eng. Online*, vol. 15, no. 1, pp. 1–11, 2016.
[24] L. Xu, M. J. Rooijakkers, C. Rabotti, J. Peuscher, and M. Mischi, "Use of power-line interference for adaptive motion artifact removal in biopotential measurements," *Physiol. Meas.*, vol. 37, no. 1, pp. 25–40, 2015.
[25] L. Xu *et al.*, "Adaptive motion-artifact reduction in capacitive ecg measurements by using the power-line interference," in *Proc. 13th Annu. IEEE Int. Symp. Med. Meas. Appl. (MeMeA)*, 2018, pp. 1–5.
[26] C. Zhan, L. F. Yeung, and Z. Yang, "A wavelet-based adaptive filter for removing ECG interference in EMGdi signals," *J. Electromyogr. Kinesiol.*, vol. 20, no. 3, pp. 542–549, 2010.
[27] G. Lu *et al.*, "Removing ECG noise from surface EMG signals using adaptive filtering," *Neurosci. Lett.*, vol. 462, no. 1, pp. 14–19, 2009.
[28] Y. Hu, X. H. Li, X. Xie, L. Y. Pang, Y. Cao, and K. Luk, "Applying independent component analysis on ecg cancellation technique for the surface recording of trunk electromyography," in *Proc. Annu. Int. Conf. IEEE Eng. Med. Biol. Soc. (EMBC)*, 2005, pp. 3647–3649.
[29] G. D. Clifford, A. H. Shoeb, P. E. McSharry, and B. Janz, "Model-based filtering, compression and classification of the ECG," *Int. J. Bioelectromagn.*, vol. 7, no. 1, pp. 158–161, 2005.
[30] E. K. Roonizi and R. Sameni, "Morphological modeling of cardiac signals based on signal decomposition," *Comput. Biol. Med.*, vol. 43, no. 10, pp. 1453–1461, 2013.
[31] G. D. Clifford, "A novel framework for signal representation and source separation: Applications to filtering and segmentation of biosignals," *J. Biol. Syst.*, vol. 14, no. 2, pp. 169–183, 2006.
[32] P. E. McSharry, G. D. Clifford, L. Tarassenko, and L. A. Smith, "A dynamical model for generating synthetic electrocardiogram signals," *IEEE Trans. Biomed. Eng.*, vol. 50, no. 3, pp. 289–294, Mar. 2003.
[33] R. Sameni, C. Jutten, and M. B. Shamsollahi, "Multichannel electrocardiogram decomposition using periodic component analysis," *IEEE Trans. Biomed. Eng.*, vol. 55, no. 8, pp. 1935–1940, Aug. 2008.
[34] J. Ben-Arie and K. R. Rao, "Nonorthogonal signal representation by Gaussians and Gabor functions," *IEEE Trans. Circuits Syst. II, Analog Digit. Signal Process.*, vol. 42, no. 6, pp. 402–413, Jun. 1995.
[35] T. K. Moon, "The expectation-maximization algorithm," *IEEE Signal Process. Mag.*, vol. 13, no. 6, pp. 47–60, Nov. 1996.
[36] L. Xu, C. Rabotti, and M. Mischi, "Characterization of a novel instrument for vibration exercise," in *Proc. Annu. Int. Conf. IEEE Eng. Med. Biol. Soc. (EMBC)*, 2012, pp. 2760–2763.
[37] A. L. Goldberger *et al.*, "Physiobank, PhysioToolkit, and PhysioNet: Components of a new research resource for complex physiologic signals," *Circulation*, vol. 101, no. 23, pp. e215–e220, 2000.
[38] L. Sörnmo and P. Laguna, "Chapter 6—The electrocardiogram—A brief background," in *Bioelectrical Signal Processing in Cardiac and Neurological Applications*. Burlington, VT, USA: Academic, 2005, pp. 411–452.
[39] Y. Xu, K. Wang, Y. Jin, F. Qiu, Y. Yao, and L. Xu, "Influence of electrode configuration on muscle-fiber-conduction-velocity estimation using surface electromyography," *IEEE Trans. Biomed. Eng.*, vol. 69, no. 8, pp. 2414–2422, Aug. 2022, doi: 10.1109/TBME.2022.3145038.
[40] J. D. M. Drake and J. P. Callaghan, "Elimination of electrocardiogram contamination from electromyogram signals: An evaluation of currently used removal techniques," *J. Electromyogr. Kinesiol.*, vol. 16, no. 2, pp. 175–187, 2006.
[41] P. Zhou and W. Z. Rymer, "Factors governing the form of the relation between muscle force and the EMG: A simulation study," *J. Neurophysiol.*, vol. 92, no. 5, pp. 2878–2886, 2004.
[42] R. Sameni, M. B. Shamsollahi, C. Jutten, and G. D. Clifford, "A nonlinear Bayesian filtering framework for ECG denoising," *IEEE Trans. Biomed. Eng.*, vol. 54, no. 12, pp. 2172–2185, Dec. 2007.